Solar Phys
DOI 10.1007/s11207-008-9134-7

# Do Photospheric Brightness Structures Outside Magnetic Flux Tubes Contribute to Solar Luminosity Variation?

**Peter Foukal · Pietro N. Bernasconi**

Received: 30 September 2007 / Accepted: 29 January 2008


**Abstract** Variations in total solar irradiance (TSI) correlate well with changes in projected area of photospheric magnetic flux tubes associated with dark sunspots and bright faculae in active regions and network. This correlation does not, however, rule out possible TSI contributions from photospheric brightness inhomogeneities located *outside* flux tubes and *spatially correlated with them*. Previous reconstructions of TSI report agreement with radiometry that seems to rule out significant "extra-flux-tube" contributions. We show that these reconstructions are more sensitive to the facular contrasts used than has been generally recognized. Measurements with the Solar Bolometric Imager (SBI) provide the first reliable support for the relatively high, wide-band, disk-center contrasts required to produce 10% rms agreement. Longer term bolometric imaging will be required to determine whether the small but systematic TSI residuals we see here are caused by remaining errors in spot and facular areas and contrasts or by extra-flux-tube brightness structures such as bright rings around sunspots or "convective stirring" around active regions.

**Keywords** Solar irradiance · Photometric imaging · Sunspots · Faculae

## 1. Introduction

Modeling of variations in total solar irradiance (TSI) has shown that fluctuations measured with space-borne radiometers correlate well with the changing areas of dark (sunspot) and bright photospheric magnetic structures (*e.g.*, Willson *et al.*, 1981; Foukal and Lean, 1988; Chapman, Cookson, and Dobias, 1996; see, *e.g.*, Solanki and Krivova, 2004, for a recent review). Such comparisons commonly report correlation coefficients $r > 0.9$ between TSI

P. Foukal (✉)
Heliophysics, Inc., 192 Willow Road, Nahant, MA 01908, USA
e-mail: pvfoukal@comcast.net

P.N. Bernasconi
Johns Hopkins University Applied Physics Laboratory, 1110 Johns Hopkins Road, Laurel, MD 20723, USA
e-mail: pietro.bernasconi@jhuapl.edu

fluctuations and area variations, over time scales between the 27-day solar rotation period and the three solar 11-year sunspot cycles now covered by space-borne radiometry (*e.g.*, Fröhlich, 2006).

These high correlations show that most ($r^2 > 80\%$) of the variance in TSI arises from brightness structures associated spatially and temporally with changing projected areas of photospheric magnetic flux tubes. However, correlation analysis alone cannot discriminate between the TSI contribution arising from the darkness of spots or the brightness of faculae versus possible contributions from brightness structures immediately surrounding these flux tubes. Examples of such "extra-flux-tube" contributions are bright rings reported around sunspots (Fowler, Foukal, and Duvall, 1983; Rast *et al.*, 1999) and possible extended, low-level brightenings around active regions associated with predicted "convective stirring" (Parker, 1995). The TSI contributions of such extra-flux-tube brightenings could elude identification, since they should be as highly correlated with the flux tubes as the "intra-flux-tube" contributions of umbrae, penumbrae, and faculae.

In principle, such extra-flux-tube contributions could be detected by subtracting the intra-flux-tube contribution (calculated from areas and contrasts of the spots and faculae) from the radiometrically measured TSI fluctuation. Any residuals should then yield signatures of an additional, extra-flux-tube contribution, if it exists. This approach requires that the intra-flux-tube contribution be known accurately enough to detect extra-flux-tube contributions at the level of roughly 10% of the sunspot deficit – the contribution level roughly predicted for spot bright rings or convective stirring brightenings.

Detection of extra-flux-tube contributions would be important, even if they accounted for only a minor part of the TSI variation on solar-rotational to multidecadal time scales. Confirmation of a contribution from sunspot bright rings would place useful constraints on the thermal diffusivity of turbulent solar convection (Spruit, 1977; Fowler, Foukal, and Duvall, 1983). Of even greater interest would be evidence for appreciable convective stirring. Such stirring lies outside the present physical understanding of solar luminosity variation, which connects TSI changes only to changes in area of photospheric magnetic flux tubes (Spruit, 1982; Foukal, Fowler, and Livshits, 1983), not to possible aerodynamic effects associated, for example, with their rate of rise (Parker, 1995). Therefore, discovery of contributions attributable to convective stirring could reopen the possibility of slower TSI variations large enough to drive climate on centennial to millennial time scales, where the correlations with solar activity are most convincing (*e.g.*, Bond *et al.*, 2001; Foukal *et al.*, 2007).

In Section 2 we discuss the factors that determine the accuracy of TSI reconstructions on time scales between solar rotation and the 11-year activity cycle. In Section 3 we discuss the three main techniques used to evaluate the facular contribution, whose uncertainty dominates the error budget of such reconstructions. Throughout this discussion we use the term "facula" to mean a bright structure whether it is located in an active region or in the surrounding enhanced network. With recent advances in facular *area* measurement, the large remaining uncertainty in facular *contrast* is the main factor that limits the accuracy of TSI reconstructions. In Section 4 we show how directly measured wide-band facular contrasts, obtained recently by using the Solar Bolometric Imager balloon-borne telescope (Foukal *et al.*, 2004; Bernasconi *et al.*, 2004), can be used to reduce this uncertainty. In Sections 5 and 6 we discuss our findings on possible extra-flux-tube TSI contributions and present our conclusions.

## 2. Factors Determining the Accuracy of Spot and Facular Contributions to TSI Reconstructions

The contribution of a spot or facula to TSI variation is given by the basic relation (Willson *et al.*, 1981; Foukal, 1981)

$$\Delta S/S = A\big[C(\mu) - 1\big]L(\mu), \tag{1}$$

where $S$ is the TSI, $A$ is the projected area of the spot or facula (expressed as a fraction of the photospheric disk), and $C$ is its photometric contrast. The limb-darkening function $L(\mu)$ gives the brightness of the undisturbed photosphere relative to disk center, at the limb distance of the spot or facula expressed in terms of $\mu$, the cosine of its heliocentric angle.

Because S represents a wide-band, pyrheliometric measurement of TSI over a spectral range between approximately 0.2 and 5 μm, the three quantities on the right-hand side of Equation (1) also should be measured in light integrated over the same broad spectral range, and with constant spectral response over that range. This requirement has never been satisfied in past reconstructions because such a "bolometric" measurement of both contrasts and also of limb darkening is beyond the capability of conventional imaging detectors. Commonly used imaging detectors respond only over limited parts of this range, and in addition, their response is generally peaked (*i.e.*, not flat) even within their wavelength range.

Since the contrast of both spots and faculae varies greatly with wavelength, the available monochromatic contrast values cannot be used in Equation (1) without significant correction. Because of this instrumental limitation, it has been necessary until now to evaluate the right-hand side of Equation (1) by using various approximations to contrast and to photospheric limb darkening, based on monochromatic measurements supplemented with theoretical modeling. The Solar Bolometric Imager (SBI) (Foukal and Libonate, 2001; Foukal *et al.*, 2004; Bernasconi *et al.*, 2004) was developed to provide the first bolometric imaging of these two quantities required for accurate modeling of TSI variation, without the uncertainty of such approximations.

In past TSI modeling, the sunspot contrasts used have been based mainly on measurements in integrated light using thermopiles (see references in Allen, 1964), although their accuracy is limited by uncertainties in atmospheric transmission and scattered light. More recent values have been obtained from model atmospheres based on spectra extending from the violet through the infrared (*e.g.*, Fontenla *et al.*, 2006). The measurement of facular contrasts is more difficult mainly because the values increase rapidly with angular resolution, since the facular elements remain unresolved with the full-disk imagers used to measure their areas. The dependence on limb distance is also more pronounced than for spots. These two factors complicate attempts to derive even reliable mononchromatic (much less wide-band) facular values from the many narrowband measurements made at different angular resolutions, wavelengths, and limb distances (*e.g.*, Libbrecht and Kuhn, 1985; Lawrence, 1988; Wang and Zirin, 1987; Foukal, Harvey, and Hill, 1991; Ortiz *et al.*, 2002). Also, in past reconstructions, the photospheric limb-darkening function, $L(\mu)$, in Equation (1) is roughly approximated by the Eddington limb-darkening relation for a gray atmosphere (Willson *et al.*, 1981; Foukal, 1981).

We consider next uncertainties in the areas. The boundaries of the large umbrae and penumbrae that cause most of the spot-induced TSI variation can be defined consistently by using photometric traces across these easily resolved structures, and their areas can now be measured to a few percent uncertainty by using dedicated photometric imagers such as the Precision Solar Photometric Telescopes (PSPT) (*e.g.*, Ermolli *et al.*, 2007) or the

Cartesian Full Disc Telescope (CFDT2; Chapman *et al.*, 1989) or with magnetograms from the National Solar Observatories or from the space-borne Michelson Doppler Imager (*e.g.*, Wenzler, Solanki, and Krivova, 2005). However, a direct measurement of facular area is not possible because the cross-sectional diameters of facular elements (*e.g.*, Lites *et al.*, 2004) lie at least an order of magnitude below the angular resolution of any available full-disk imagers or magnetographs.

In summary, we see that neither the true areas of faculae nor their true contrast is accessible to TSI modeling. Fortunately, we are able to show here that, if our aim is to measure the *contribution to TSI* of a spot or facula, we do not necessarily require the true areas or true contrasts of these structures. We proceed as follows: The contribution $\delta S$ to TSI from a structure of brightness $B$ and subtending a small solid angle $\delta\omega$ is essentially independent of the angular resolution used, since it is always given by

$$\delta S = B\delta\omega. \tag{2}$$

The value of $\delta S$ will be the same whether it is measured at high angular resolution ($\delta\omega$ small and $B$ large) or with greater instrumental blurring that decreases $B$ but increases $\delta\omega$ (through convolution) by the same relative amount. The important consideration is to measure both the contrast and solid angle with the *same* angular resolution. Of course, the resolution must be sufficient to prevent so much blurring that the darkening of a spot or facular brightening can no longer be measured with adequate ($\sim 10\%$) photometric precision against detector and granulation noise. This resolution requirement is easily satisfied, even for the smallest facular structures in decaying active regions, known to contribute to TSI variation. Photometric imaging with dedicated instruments such as the PSPT or the CFDT2 takes advantage of the improved accuracy of measuring both quantities with the same instrument.

However, even if such spatial resolution errors are minimized, these conventional imagers do not provide bolometric response, so the contrasts still must be corrected to their wide-band values. These corrections can be large and uncertain. Taking the (better known) bolometric corrections for umbrae as a guide, we note that the wide-band umbral relative intensity near disk center is calculated to be about 24% (*e.g.*, Allen, 1964), whereas the measured monochromatic values increase from about 5% in the blue to almost 60% in the infrared (Cox, 2000). Therefore, an estimate of the umbral contribution to TSI variation based on an uncorrected narrowband measurement could be in error by a factor of two. Errors of similar size can be expected for faculae.

In principle, bolometric corrections could be roughly estimated by assuming, for example, Planckian radiation from faculae and the photosphere. The monochromatic contrast could then be used to calculate the excess in color temperature for the facula, and thence its excess blackbody radiation. Lawrence (1988) showed that such a Planckian approximation holds reasonably well in the green and red. However, its accuracy in estimating the total, broadband facular contribution to TSI was only demonstrated recently by bolometric imaging (Foukal *et al.*, 2004; see also Ermolli *et al.*, 2007), and we are not aware of its use in any published TSI reconstruction so far.

## 3. The Accuracy of Reconstructed Facular Contributions to TSI Variation

Three basic approaches have been devised to avoid the difficulties with evaluation of facular area and contrast as identified here. In the first the sunspot contribution to the right-hand side of Equation (1), called the Photometric Sunspot Index (PSI), is subtracted from the radiometrically measured left-hand side of Equation (1). The residuals, (TSI – PSI), are found to correlate well with various indices of facular area and brightness such as the microwave flux, F10.7, the helium index He 10830, the Lyman alpha flux, or even the sunspot number. A regression curve of the (TSI – PSI) residuals versus such an index is constructed by using data over a period when TSI radiometry, sunspot areas, and the facular index are all available. If the relation is assumed to be stable in time, this regression can then be used to reconstruct the facular contribution to TSI whenever the facular index is available. The contribution (TSI – PSI) can then be added back to PSI to yield the reconstructed value of (TSI − PSI) + PSI = TSI for any day when PSI can be calculated from sunspot statistics.

This technique, or modifications extended to multiple regressions, has been widely used to identify the TSI contribution of faculae in active regions (Foukal and Lean, 1986; Chapman, Cookson, and Dobias, 1996) and of network (Foukal and Lean, 1988; Fröhlich and Lean, 2004) and to reconstruct the TSI variation back to the Maunder Minimum (*e.g.*, Foukal and Lean, 1990; Solanki and Fligge, 1999). The good correlation between the residuals and facular indices, when obtained by using such *full-disk* proxies, provides a TSI reconstruction that avoids errors in facular areas and contrasts. However, such studies do not distinguish between the contribution of faculae versus possible extra-flux-tube contributions that might also be correlated with the same facular indices.

In a second approach, narrowband measurements have been used to approximate bolometric facular contrasts. In the most comprehensive such study, Lean *et al.* (1998) used the measurements of Lawrence (1988) and Libbrecht and Kuhn (1985) to bracket the range of facular contrast behavior. (The Lawrence values increase toward the limb whereas the Libbrecht and Kuhn values decrease.) Lean *et al.* found that the TSI reconstruction was insensitive to which near-limb behavior is adopted.

However, their analysis overlooks the sensitivity of TSI to the values of facular contrast further from the limb. These values, at $\mu > 0.4$, apply over most of the disk, where the projected area of faculae is largest. The values adopted by Lean *et al.* are shown in Figure 1

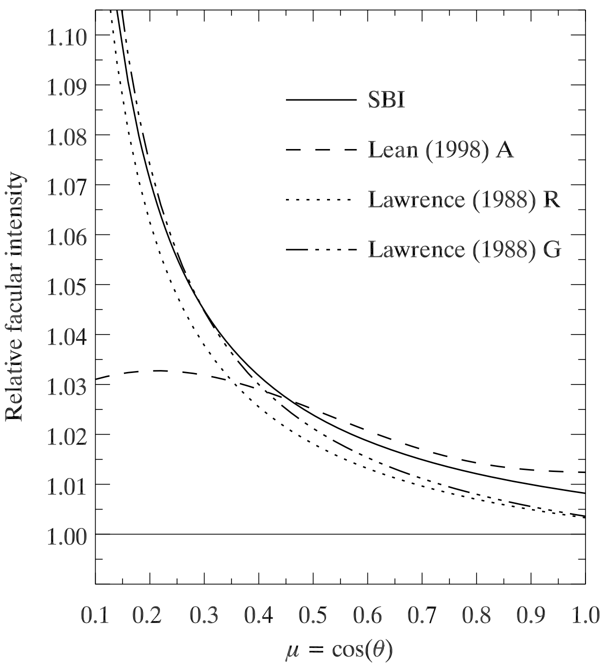


**Figure 1** A plot of facular contrast versus $\mu$ (cosine of heliocentric angle). The two monochromatic (0.15-nm passband) curves measured by Lawrence (1988) at 524.5 (dot-dashed) and 626.4 nm (dotted) are labeled G, and R, respectively. The curve adopted by Lean *et al.* (1998) is shown dashed. The bolometric curve measured with the SBI (Foukal *et al.*, 2004) is shown as a solid line.

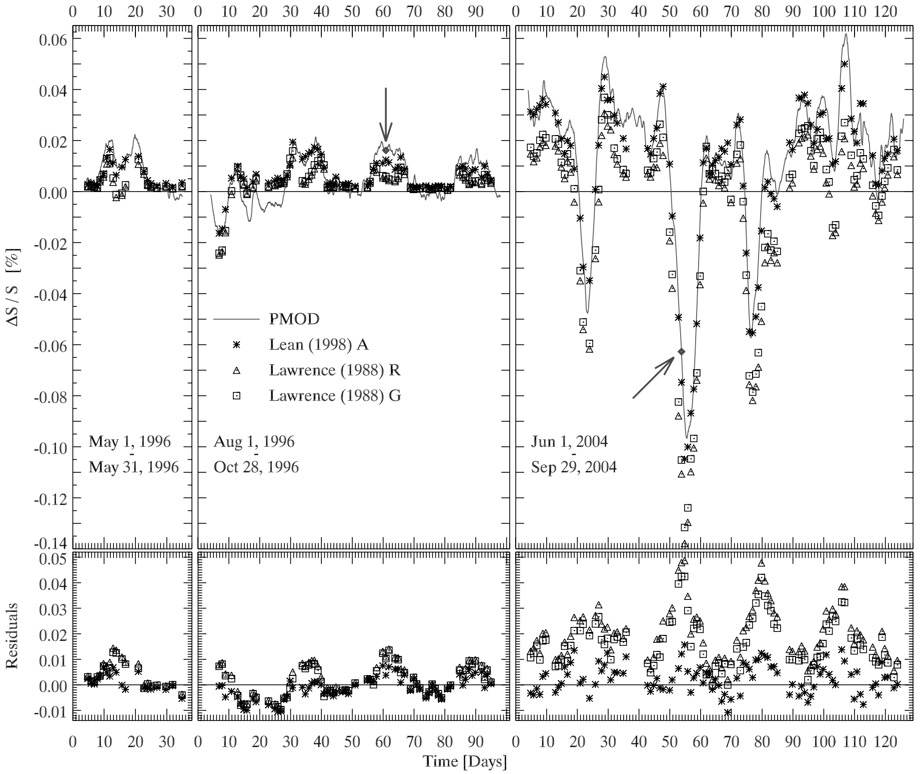


**Figure 2** Upper panels: A plot of TSI reconstructed by using the two facular contrast curves plotted in Figure 1, measured by Lawrence (1988) (triangles and squares) and that adopted by Lean *et al.* (1998) (stars), for comparison with the PMOD composite (solid line). Three periods are reconstructed: 1 – 31 May and 1 August – 28 October 1996, and 1 June – 29 September 2004. The arrows point at the radiometry measurements for the dates of the images shown in Figure 4. Lower panels: The residuals (PMOD – model) for these reconstructions. All ordinates are in percentage of TSI.

for comparison with those actually observed by Lawrence in narrow red and green bands. (Libbrecht and Kuhn's values are not shown, since they only measured very near the limb.) We see that the contrasts adopted by Lean *et al.* exceed the observed values by up to a factor of three near disk center.

Figure 2 shows TSI reconstructed by using the facular contrasts adopted by Lean *et al.* for comparison with TSI reconstructed by using the actual Lawrence measurements. (In Section 4 we describe the method we used to reconstruct the measured TSI from the facular curves shown in Figure 1.) Three periods are shown here: two in 1996 when spots made a negligible contribution to TSI and a third in 2004 when large spots contributed significantly to TSI variation. From the residuals plotted there, and from their rms values given in Table 1, we see that the amplitude agreement between the variations seen in the radiometry and in the reconstruction is much better ($< 10\%$) when the higher contrasts chosen by Lean *et al.* are used than when the actual contrasts measured by Lawrence are used (only $\sim 30\%$). The Lawrence and Libbrecht and Kuhn measurements were made in restricted visible passbands, so the actual uncertainty is even larger, since no bolometric corrections were provided.

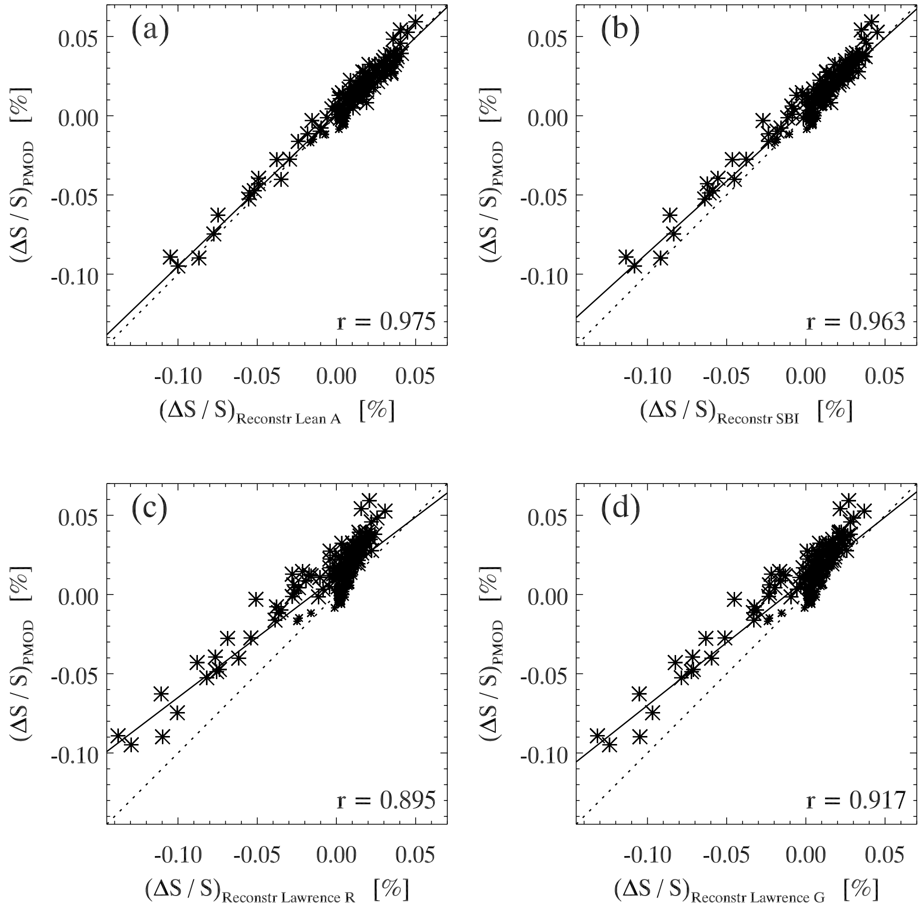


**Figure 3** Scatter plots of PMOD TSI composite in percentage of $S$ (ordinates) versus TSI reconstructed by using facular contrasts: (a) adopted by Lean *et al.* (1998); (b) measured by SBI; (c, d) measured in red, green by Lawrence (1988). The solid line represents a linear regression fit to the data. The dashed line denotes unity slope.

Figures 3a, 3c, and 3d show scatter plots of the radiometry versus TSI reconstructed by using the same three curves. We see that the correlation is higher when the higher contrasts at $\mu > 0.4$ adopted by Lean *et al.* are used. These results indicate that both the reported 10% amplitude agreement and also the highest correlation are only obtained if disk facular contrasts up to three times higher than those they referenced are used. The Lean *et al.* result was interesting in being one of the first to show that a facular contrast curve can be found that provides a good fit to the TSI variation over a four-year period spanning a wide range of solar activity. However, their study left open how well the curve they adopted agreed with an actual curve of bolometric facular contrast.

A third approach is to *calculate* the facular contrasts by using semiempirical models of facular atmospheres (*e.g.*, Fligge, Solanki, and Unruh, 2000; Fontenla, Harder, and Rottman, 2004; Penza *et al.*, 2004; Wenzler, Solanki, and Krivova, 2005; Wenzler *et al.*, 2006). Such a calculation can be useful, for example, in estimating the spectral dependence of facular contrast (and therefore in solar spectral irradiance variability) in certain poorly observed wavelength regions important to aeronomy. However, Krivova *et al.* (2003) state candidly that the good agreement reported in TSI reconstructions based on such an approach is achieved by *adjusting the facular contrast curve to produce optimum agreement with the TSI radiometry*. Once adjusted, the curve is kept constant over the period of the reconstruction, so the good fit achieved suggests, as in the Lean *et al.* (1998) study, that photospheric magnetic structures *might* account for most of the measured TSI variation over rotational time scales and also over an entire solar cycle.

This ability to reproduce TSI variation over a range of time scales and also other agreements reported between modeled and observed Fraunhofer lines and in area filling factors of facular elements have been put forward as evidence for the correctness of the chosen facular contrast behavior (*e.g.*, Krivova *et al.*, 2003; Solanki and Krivova, 2004). Although this agreement is encouraging, it does not constitute a quantitative inquiry into the sensitivity of the TSI reconstruction to any of these parameters. Given the sensitivity of TSI to facular contrast shown here, it remains to be shown that these agreements provide meaningful constraints on the accuracy of the reconstruction. Also, we need to examine how well such a "chosen" facular contrast curve agrees with photometric observations of faculae.

The data given by Ermolli *et al.* (2007) in their Figure 12 show that even the narrowband facular contrasts calculated from such facular atmosphere models agree only very roughly ($\pm 30\%$) with available narrowband facular photometry (see also Unruh, Solanki, and Fligge, 2000). A bolometric contrast curve calculated from the same model atmospheres (Unruh, 2007) also falls within this rough general range. However, given the sensitivity of reconstructed TSI variation to facular contrast illustrated in Figure 2, such rough agreement is insufficient to evaluate the intra-flux-tube contribution to 10% and decide whether an extra-flux-tube contribution exists. The most reliable way to obtain the wide-band contrast of faculae required in Equation (1) is to measure it directly with a bolometric imager.

## 4. A TSI Reconstruction Using Broadband Measurements of Facular Contrast

The first bolometric measurements of broadband facular contrast were obtained by using the SBI balloon telescope on 1 September 2003 (Foukal *et al.*, 2004; Bernasconi *et al.*, 2004). A curve showing the center-to-limb behavior of wide-band facular contrast is shown in Figure 1. Our values lie above the narrowband measurements of Lawrence (1988), but they agree reasonably well when Lawrence's narrowband measurements are corrected to bolometric values by assuming Planckian radiation from the photosphere and faculae (Foukal *et al.*, 2004). This agreement between two independent measurement sets at similar angular resolution increases our confidence in these first SBI results. The SBI broadband contrasts lie somewhat below the values adopted by Lean *et al.* (1998), over the range $\mu > 0.4$. Closer to the limb, they lie well above them.

The SBI also produced the first broadband measurement of the photospheric limb-darkening curve required for accurate evaluation of the right-hand side of Equation (1). In our reconstruction, this limb-darkening function can be expressed as

$$L(\mu) = a + b\mu + c\mu^2 + d\mu^3, \tag{3}$$

where the coefficients $a = 0.435$, $b = 0.694$, $c = -0.129$, and $d = 3.75 \times 10^{-4}$ have been evaluated from the broadband limb-darkening curve measured with the SBI (Foukal *et al.*, 2004).

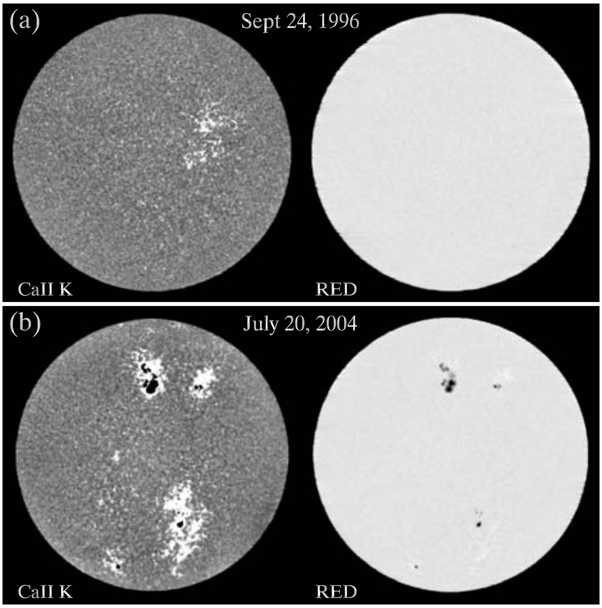


**Figure 4** Images taken with the CFDT2 of the appearance of spots and faculae on the solar disk on (a) 24 September 1996, and (b) 20 July 2004, illustrating the two periods of facula- and spot-dominated TSI variation, respectively. The Ca II K narrowband images used to choose the facular pixels appear to the left, and the red continuum images used to measure spot areas are shown on the right. The reconstructed TSI values for these two days are indicated by arrows in Figure 2.

The sunspot contribution to $\Delta S$ is calculated separately for umbrae and penumbrae by using their individually measured areas and the most recent values for their contrasts, $C_{\mathrm{s}} =$ 0.21 and 0.83, respectively (Fontenla *et al.*, 2006). These contrasts are assumed here to be independent of $\mu$.

The facular contribution is calculated by using the contrast function

$$C_{\mathrm{f}}(\mu) = \left[(a/\mu) - b\right] + 1, \tag{4}$$

where the coefficients of broadband facular limb darkening, $a = 0.0157$ and $b = 0.0075$, have been obtained from the SBI measurements.

Figure 4 shows the appearance of the spots and faculae on the disk during typical days during the periods of low and high activity in 1996 and 2004 chosen for our reconstruction. These images were obtained at the San Fernando Observatory with the CFDT2 photometric telescope (Chapman *et al.*, 1989). The relatively low angular resolution CFDT2 data were chosen to minimize differences in the blurring of spot and facular areas by the point response of the SBI and CFDT2. The scale of decaying plage remnants, which comprise the smallest magnetic structures known to influence TSI variation, is roughly 10 arcsecs. The difference between the blurring by the convolutions of such a structure with the SBI and CFDT2 point-response functions is less than 10%. The areas $A$ were measured from daily CFDT2 images at a scale of 2.5 arcsecs per pixel. The umbral and penumbral areas were measured from images taken in a 10-nm continuum passband at 672.3 nm, and the facular areas were determined from images through a 1-nm bandpass filter centered on the Ca II K line at 393.4 nm. Figure 5 shows contours illustrating the umbral, penumbral, and facular areas measured in a large active region on 20 July 2004.

The data reduction followed the procedure described by Walton *et al.* (1998). This reduction corrects for optical distortions, raster effects, and limb darkening. The photometric contrast thresholds used to select umbral and penumbral pixels were 0.68 and 0.91, respectively. These were based on previous studies by G. Chapman and J. Lawrence of the

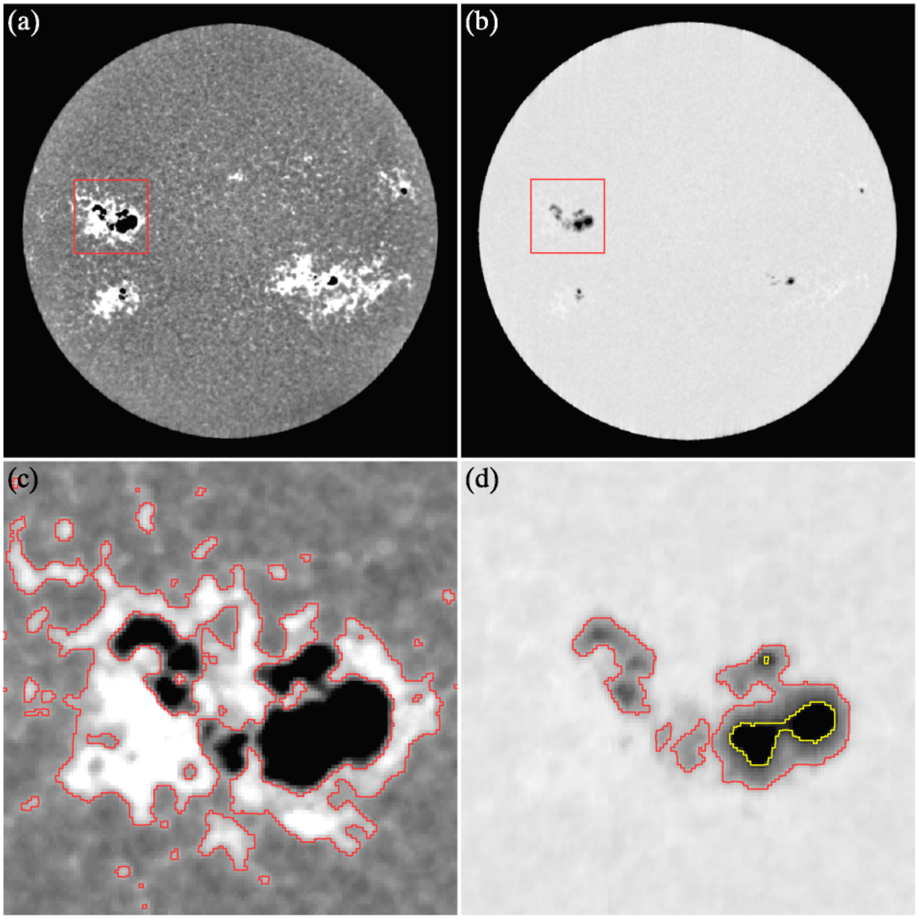


**Figure 5** CFDT2 images on 20 July 2004 (as in Figure 4) in (a) Ca K and in (b) red continuum together with contours showing areas measured for (c) facula area and (d) spot area in the large active region marked with a square in panels (a) and (b).

inflection points in tracings across spots using the SFO 24″ aperture vacuum telescope. The facular threshold of 1.05 represents three times the standard deviation of the pixel intensity distribution on flat-fielded CFDT2 images. This value has been used in many past SFO studies of faculae (*e.g.*, Chapman, Cookson, and Dobias, 1996). The daily value of TSI was calculated by summing the individual contributions found from Equation (1) for each individual spot and facula on the disk. The result was compared with the radiometric TSI value for that day, as provided by the PMOD composite record (Fröhlich, 2006) mostly obtained from VIRGO data. We normalized each TSI measurement to the quiet-Sun TSI value of 1365.34 $\mathrm{W\,m^{-2}}$.

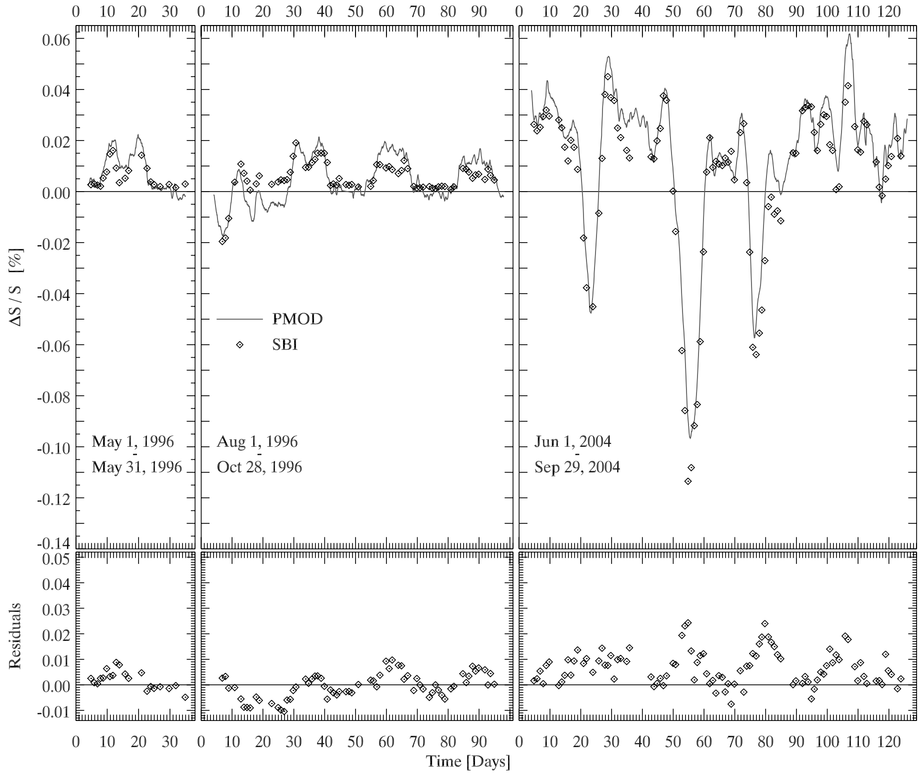


**Figure 6** Same as Figure 2, but showing the TSI reconstruction and residuals (PMOD – reconstruction) obtained by using the measured SBI facular contrasts (diamonds) for comparison with the radiometry (solid line).

## 5. Results and Errors

Figure 6 shows TSI reconstructed by using the SBI facular contrast curve for comparison with the radiometry. We see in the top panels that the SBI-based reconstruction agrees well with the radiometry. The correlation coefficient is 0.96 for the entire 1996 and 2004 data set. The residuals (TSI − model) plotted in the lower panels illustrate the agreement in *amplitude*. During 1996, the rms (in percentage of TSI) of the residuals (Table 1) was below 0.005. In 2004 they are below 0.01, corresponding to a scatter of about 10% rms relative to the peak-to-peak TSI variation, which is dominated by large spots.

This scatter is consistent with the roughly 10% agreement reported by Lean *et al.* (1998) in their reconstruction of TSI over a longer period between 1991 and 1995. The two studies used independent approaches to measuring areas in these two different time periods – one based on imaging from the CFDT2 at SFO and the other using flat fields and thresholds appropriate to images from Big Bear Solar Observatory. So the details and uncertainties of area measurement seem to be less important in achieving agreement than the choice of facular contrast curve.

We see from Figures 1, 2, and 6 that relatively high facular contrast values at $\mu > 0.4$ are required to achieve agreement with the radiometry. That is, the residuals shown in Figure 2 are about twice as large as those shown in Figure 6, and they reach 30 – 50% of the TSI

**Table 1** The rms and mean values of the residuals (TSI – model).

| Reconstruction | Time period | rms | Mean |
|---|---|---|---|
| SBI | 1996 May | 0.0039 | 0.0019 |
| | 1996 August – October | 0.0049 | −0.0005 |
| | 2004 June – September | 0.0094 | 0.0067 |
| Lean *et al.* (1998) A | 1996 May | 0.0035 | 0.0013 |
| | 1996 August – October | 0.0045 | −0.0012 |
| | 2004 June – September | 0.0061 | 0.0026 |
| Lawrence (1988) Green | 1996 May | 0.0059 | 0.0037 |
| | 1996 August – October | 0.0059 | 0.0013 |
| | 2004 June – September | 0.0192 | 0.0166 |
| Lawrence (1988) Red | 1996 May | 0.0068 | 0.0045 |
| | 1996 August – October | 0.0062 | 0.0020 |
| | 2004 June – September | 0.0228 | 0.0203 |

variation near the minima of the three largest sunspot-induced dips of TSI. Neither our reconstruction for 1996 – 2004 nor the Lean *et al.* reconstruction for 1991 – 1995 would have achieved 10% agreement with radiometry using the lower values measured by Lawrence (1988). Therefore, our study is the first in which the relatively high facular contrasts on the disk required for close agreement with the radiometry are supported by actual broadband photometric measurements of faculae.

Figure 6 shows systematically positive residuals over four solar rotations at high activity levels in 2004 and proportionately smaller, but still mainly positive, residuals over four solar rotations at lower activity levels in 1996. These might indicate an extra-flux-tube TSI contribution from bright structures not included in our reconstruction. However, evaluation of such residuals must take into account that the SBI facular contrasts refer to the wavelength range above the (balloon) atmospheric cutoff around 310 nm, whereas the radiometry includes the UV contribution down to roughly 200 nm. This 200-nm cutoff is expected because of photoelectron emission from carbon blacks. The 200 – 300 nm range is estimated to contribute about 20 – 30% of the TSI variation over a solar cycle (*e.g.*, Lean, 1989; Unruh and Solanki, 1998).

Previous studies (*e.g.*, Foukal and Lean, 1988) have shown that the actual TSI increase is about twice the net 11-year TSI modulation. Since the 20 – 30% UV contribution was calculated as a fraction of net TSI modulation, it represents about 10 – 15% of the bright component TSI contribution. To within present uncertainties in the 200 – 310 nm response of cavities and of the SBI, this correction may help to account for the mainly positive residuals.

Remaining uncertainties in sunspot and facular contrasts and areas may also play a role in determining the sign of these residuals. However, we performed the reconstructions using two other sets of umbral and penumbral contrasts given by Allen (1964, 1973), and the positive residuals remained. The quiet value of TSI was chosen as the PMOD value during the two most quiet periods around solar activity minimum in 1996, seen in the second panels of Figures 2 and 6. Error in this value should have little effect on the residuals, since the reconstruction is calculated simply as a fractional variation of this adopted quiet-Sun value.

## 6. Discussion and Conclusions

We show here that TSI variation can be reconstructed to about 10% agreement on solar rotational time scales, from the changing projected areas of spots and faculae. Similar or better agreement has been reported for many past reconstructions over longer time scales extending to an 11-year cycle, so it is important to understand the advance presented here.

Our TSI reconstruction is the first to use actual *measured broadband facular contrasts* required to evaluate Equation (1), rather than uncertain approximations based on monochromatic photometry of faculae or on calculations using facular atmospheres. We show that the sensitivity of the TSI reconstruction to the facular contrast curve is significantly greater than has been previously stated.

Given this sensitivity, the choice of facular contrast curve is critical to the agreement in amplitude achieved between the reconstruction and the radiometry. In the Lean *et al.* (1998) study, the facular contrast values adopted over most of the disk exceeded the measured values referenced in that study by up to a factor of three near disk center. If the actual measured values of Lawrence (1988) had been used, the agreement with radiometry, as measured by these residuals, would have been no better than 30%. In our study, the relatively high contrasts required to achieve 10% agreement have been measured directly.

In reconstructions based on calculated facular contrasts, agreement is achieved (see, *e.g.*, Krivova *et al.*, 2003) by adjusting the facular contrast curve to achieve optimum agreement with the radiometry. Various indirect arguments have been presented by these authors to justify this adjustment, including the models' success in reproducing total and spectral irradiance variations on both solar rotational and 11-year time scales. These agreements are encouraging, but in the absence of any error analysis showing the precision of these constraints, it seems difficult to assign an accuracy to these TSI reconstructions.

The third type of reconstruction, based on correlation with full-disk facular proxies, avoids errors from uncertain facular areas and contrasts but is inherently ill-suited to distinguishing intra-flux-tube contributions to TSI from extra-flux-tube contributions also correlated both spatially and temporally with facular proxies.

The agreement found here indicates that additional contributions to solar luminosity variation originating *around* active regions probably account for less than about 10% of the TSI variation, at least on the time scales of solar rotation studied here. This agreement is *consistent* with the physical explanation of solar luminosity variation caused by photospheric magnetic flux tubes (Spruit, 1982; Foukal, Fowler, and Livshits, 1983). However, the effective thermal diffusivity of the solar convective layers and also the depth and dynamics of such magnetic structures as spots and faculae are not sufficiently well known to predict accurately the contribution of sunspot bright rings (Spruit, 1977; Fowler, Foukal, and Duvall, 1983). Identification of a bright ring contribution would therefore provide interesting constraints on these parameters of solar magneto-convection.

The theory alone cannot rule out the possible contribution of additional aerodynamic effects on convection ("convective stirring") conceivably associated with rising active region flux tubes (Parker, 1995), although any effects of such stirring would tend to be damped by the enormous thermal inertia of subphotospheric layers (Spruit, 1982; Foukal *et al.*, 2007). Identification of such aerodynamic effects, even if they were minor on solar rotational time scales, would open new possibilities for larger TSI variations of climatological importance on longer centennial to millennial time scales.

Imaging of *both* areas and contrasts with the same SBI instrument over a period of at least several solar rotations will be necessary to provide the homogeneous data set required to determine whether the systematically positive residuals we see are caused by, for example, uncertainties of spot and facular areas and contrasts or by more interesting possibilities such as sunspot bright rings or convective stirring. The required accuracy cannot be achieved with the one day of SBI measurements available here. Rings of 3% amplitude reported by Rast *et al.* (1999) could cancel about 10% of the spot radiative deficit and thus explain the sense and magnitude of the residuals seen here. However, only much weaker rings were reported in an earlier study of comparable sensitivity by Fowler, Foukal, and Duvall (1983).

A first step toward achieving this next level of precision would have been the SBI flight on a long-duration balloon in Antarctica in December 2006. Unfortunately, this flight was not successful. A successful recent one-day flight from Ft Sumner, New Mexico, in September 2007 provides a good baseline at low activity levels. It opens the way to observations at higher activity levels with a possible longer balloon flight from Kiruna, Sweden, in 2008 and a space-borne SBI being proposed for flight in the forthcoming round of Small Explorer (SMEX) missions. Such a space-borne SBI flown together with radiometers would enable accurate removal of both the sunspot and facular TSI contributions over a substantial part of a solar cycle. This advance would help determine whether additional contributions from sources other than photospheric magnetic activity affect TSI over multidecadal to millennial time scales of direct importance to climate.

**Acknowledgements** We acknowledge early contributions to this paper from the late Stephen Walton. We are also grateful to D. Rust for his comments on this paper and H. Eaton for his many engineering contributions to the SBI program. We thank PMOD/WRC, Davos, Switzerland, for making available the PMOD TSI composite (version 6-000-0412) and we extend our thanks also to the VIRGO team for unpublished data from the VIRGO experiment on the cooperative ESA/NASA mission SOHO. We thank Y. Unruh for calculating a bolometric contrast curve from her model atmospheres. This work was supported by NASA Grant Nos. NNG05WC07G and NAG5-10998 (PNB and PVF) and by NSF Grant No. ATM-0718305 (PVF).

## References

Allen, C.W.: 1964, *Astrophysical Quantities*, 2nd edn. The Athlone Press, London.
Allen, C.W.: 1973, *Astrophysical Quantities*, 3rd edn. The Athlone Press, London.
Bernasconi, P.N., Eaton, H.A.C., Foukal, P., Rust, D.M.: 2004, *Adv. Space Res.* **33**, 1746.
Bond, G., Kroner, B., Beer, J., Muscheler, R., Evans, M.N., Showers, W., Hoffmann, S., Lotti-Bond, R., Hajdas, I., Bonani, G.: 2001, *Science* **294**, 2130.
Chapman, G.A., Cookson, A.M., Dobias, J.J.: 1996, *J. Geophys. Res.* **101**, 13541.
Chapman, G.A., Herzog, A.D., Laico, D.E., Lawrence, J.K., Templer, M.S.: 1989, *Astrophys. J.* **343**, 547.
Cox, A. (ed.): 2000, *Allen's Astrophysical Quantities*, 4th edn. Springer, New York.
Ermolli, I., Criscuoli, S., Centrone, M., Giorgi, F., Penza, V.: 2007, *Astron. Astrophys.* **465**, 305.
Fligge, M., Solanki, S.K., Unruh, Y.: 2000, *Astron. Astrophys.* **353**, 380.
Fontenla, J., Harder, J., Rottman, G.: 2004, *Astrophys. J.* **605**, L85.
Fontenla, J., Avrett, E., Thuillier, G., Harder, J.: 2006, *Astrophys. J.* **639**, 441.
Foukal, P.: 1981, In: Cram, L., Thomas, J. (eds.) *The Physics of Sunspots*, Sacramento Peak Observatory, Sunspot, 391.
Foukal, P., Lean, J.L.: 1986, *Astrophys. J.* **302**, 826.
Foukal, P., Lean, J.L.: 1988, *Astrophys. J.* **328**, 347.
Foukal, P., Lean, J.: 1990, *Science* **247**, 556.
Foukal, P., Libonate, S.: 2001, *Appl. Opt.* **40**, 1138.
Foukal, P., Fowler, L.A., Livshits, M.: 1983, *Astrophys. J.* **267**, 863.
Foukal, P., Harvey, K., Hill, F.: 1991, *Astrophys. J.* **383**, L89.
Foukal, P., Bernasconi, P.N., Eaton, H.A.C., Rust, D.M.: 2004, *Astrophys. J.* **611**, L57.
Foukal, P., Fröhlich, C., Spruit, H., Wigley, T.: 2007, *Nature* **443**, 161.
Fowler, L.A., Foukal, P., Duvall, T.: 1983, *Solar Phys.* **84**, 33.
Fröhlich, C.: 2006, *Space Sci. Rev.* **125**, 53.
Fröhlich, C., Lean, J.: 2004, *Rev. Astron. Astrophys.* **12**, 273.
Krivova, N.A., Solanki, S.K., Fligge, M., Unruh, Y.C.: 2003, *Astron. Astrophys.* **399**, L1.
Lawrence, J.: 1988, *Solar Phys.* **116**, 17.

Lean, J.: 1989, *Science* **244**, 197.
Lean, J.L., Cook, J., Marquette, W., Johannesson, A.: 1998, *Astrophys. J.* **492**, 390.
Libbrecht, K., Kuhn, J.: 1985, *Astrophys. J.* **299**, 1047.
Lites, B., Scharmer, G.B., Berger, T.E., Title, A.M.: 2004, *Solar Phys.* **221**, 6.
Ortiz, A., Solanki, S.K., Domingo, V., Fligge, M., Sanahuja, B.: 2002, *Astron. Astrophys.* **388**, 1036.
Parker, E.N.: 1995, *Astrophys. J.* **440**, 415.
Penza, V., Caccin, B., Ermolli, I., Centrone, M.: 2004, *Astron. Astrophys.* **413**, 1115.
Rast, M.P., Fox, P.A., Lin, H., Lites, B.W., Meisner, R.W., White, O.R.: 1999, *Nature* **401**, 678.
Solanki, S.K., Fligge, M.: 1999, *Geophys. Res. Lett.* **26**, 2465.
Solanki, S.K., Krivova, N.A.: 2004, *Solar Phys.* **224**, 197.
Spruit, H.C.: 1977, *Solar Phys.* **55**, 3.
Spruit, H.C.: 1982, *Astron. Astrophys.* **108**, 348.
Unruh, Y.: 2007, Private communication.
Unruh, Y., Solanki, S.K.: 1998. In: Donahue, R.A., Bookbinder, J.A. (eds.) *Cool Stars, Stellar Systems and the Sun*, *ASP Conf. Series* **154**.
Unruh, Y., Solanki, S.K., Fligge, M.: 2000, *Space Sci. Rev.* **94**, 139.
Walton, S.R., Chapman, G.A., Cookson, A.M., Dobias, J.J., Preminger, D.G.: 1998, *Solar Phys.* **179**, 31.
Wang, H., Zirin, H.: 1987, *Solar Phys.* **110**, 281.
Wenzler, T., Solanki, S.K., Krivova, N.A.: 2005, *Astron. Astrophys.* **432**, 1057.
Wenzler, T., Solanki, S.K., Krivova, N.A., Fröhlich, C.: 2006, *Astron. Astrophys.* **460**, 583.
Willson, R.C., Gulkis, S., Janssen, M., Hudson, H.S., Chapman, G.A.: 1981, *Science* **211**, 700.